Journal of Inclusion Phenomena and Macrocyclic Chemistry **45:** 241–249, 2003.

Azacrownlactams Derived from Biphenyl. Study of Their Conformations, Complexation Ability and Electrochemical Behavior

A.M. COSTERO[1]*, M.J. AURELL[1], M.J. BAÑULS[1], L.E. OCHANDO[2], F.J. TAMARIT[2] and A. DOMENECH[3]

[1]*Departamento de Química Orgánica, Facultad de Química, Universidad de Valencia;* [2]*Departamento de Geología, Facultad de Química, Universidad de Valencia;* [3]*Departamento de Química Analítica, Facultad de Química, Universidad de Valencia, Doctor Moliner 50, 46100-Burjassot, Valencia, Spain*

(Received 14 May 2002; in final form: 6 February 2003)

Key words: azacrownlactams, biphenyl, complexation, electrochemistry

Abstract

Several macrolactams containing in their structure biphenyl and pyridine moieties have been synthesized. The complexation ability of these compounds has been evaluated and the results have been explained considering the existence of intramolecular hydrogen bonds. Conformational studies have been developed in some cases. Single-crystal X-ray diffraction studies have been carried out with one of the ligands. The electrochemical response of ligands **1** and **3** has been studied using cyclic and square wave voltammetry. The interaction of these ligands with Cu^{2+} ions in CH_3CN has been investigated by electrochemical techniques.

Introduction

Crown ethers derived from biphenyl have been widely used with different goals. Thus 6,6′-dimethyl-19-crown-5 and 6,6′-dimethylbiphenyl-21-crown-7 were prepared by Rebek [1] and used as controls in his studies on allosteric cooperativity. Other related compounds were used by Diederich to carry out experiments on chiral recognition in an aqueous solution [2]. Lately, Finney *et al.* have reported the synthesis of fluorescent chemosensors based on conformational restriction of a biphenyl crown ether derivative [3]. All these applications are really based on the rigidity of the biaryl framework that fixes the dihedral angle defined by the aromatic rings when a complex has been formed. During the last years our research group has been working on the synthesis of crown ether and azacrown ether derivatives covalently attached to the 2,2′ position of a 4,4′-bis(dimethylamino)biphenyl [4]. The fluorescent and electrochemical properties of the synthesized compounds have been studied and some of them have shown utility as fluorescent sensors [5]. Due to the flexibility of the crown chain, most of the prepared ligands show a poor electrochemical response. Taking into account the previously obtained results we now report the synthesis, complexation and electrochemical behavior of more rigid ligands derived from 4,4′-bis(dimethylamino)biphenyl. The newly designed compounds contain in their structures amide groups and pyridine rings. These building blocks were chosen as pyridine-amide-based macrocycles preorganize their binding sites due to hydrogen bonding or conformational rigidity [6].

* Author for correspondence. E-mail: Ana.Costero@uv.es

Experimental section

General methods

All commercially available reagents were used without further purification. Air- and humidity-sensitive reactions were performed in flame-dried glassware under argon. Column chromatography was carried out on SDS 60 A-CC silica gel and on Scharlau activated neutral aluminium oxide (activity grade 1). Melting points were measured with a Cambridge Instrument and a Reichter Termovar. NMR spectra were recorded with Bruker AC-300 and Varian Unity-300/400 spectrometers. Chemical shifts were reported in parts per million downfield from TMS. Spectra taken in $CDCl_3$ were referenced to either TMS or residual $CHCl_3$. When the spectra were recorded in CD_3CN, the residual solvent was taken as reference. Mass spectra were taken with a VG-AUTOSPEC mass.

Synthesis of dinitromacrocycle **1**. *General procedure*

Two solutions were prepared: A) Solution of 2,6-pyridinedicarboxamide **7** (0.279 g, 1.1 mmol) in dry CH_2Cl_2 (18 ml) and B) Solution of 4,4′-dinitrobiphenyl-2,2′-dicarbonyl dichloride (0.406 g, 1.1 mmol) in dry CH_2Cl_2 (18 ml). Both solutions were added dropwise with the same speed for 20 minutes to a stirred ice-cooled mixture of anhydrous K_2CO_3 (0.692 g, 5 mmol) and tetrabutyl ammonium iodide (4 mg) in dry CH_2Cl_2 (165 ml); then stirring was continued at room temperature. After completion of the reaction (TLC, 5 days), the suspension was filtered off and the residue was washed with AcOEt. The solvents were

removed from the combined filtrate and washings and the crude reaction product was chromatographed on alumina neutral column using CH_2Cl_2- metanol (97 : 3) mixture as an eluent to isolate macrocycle **1** as a white solid (0.1909 g, 35 %); mp 265–267 °C; IR (KBr) ν_{max}: 3400 (NH), 3110 (Ar—H), 2950 (CH_2), 1745 (C=O), 1690 (N—C=O), 1630 (O—N=O), 1575 (NO_2), 1300–1050 (COO, NO_2) cm^{-1}. ^1H NMR ($CDCl_3$) δ (ppm): 8.73 (2H, d, J = 2.4 Hz, Ar—H), 8.40 (2H, dd, J_1 = 2.4 Hz, J_2 = 8.4 Hz, Ar—H), 8.29 (2H, d, J = 7.7 Hz, Py—H), 8.01 (1H, t, J = 7.7 Hz, Py—H), 7.88 (2H, bt , J = 5.7 Hz, HN—CO), 7.41 (2H, d, J = 8.4 Hz, Ar—H), 4.61–4.54 (2H, ddd, J_1 = 2.3 Hz, J_2 = 8.6 Hz, J_3 = 11.7 Hz, O—CH_2—), 4.30–4.23 (2H, ddd, J_1 = 2.4 Hz, J_2 = 5.3 Hz, J_3 = 11.7 Hz, O—CH_2—), 3.89–3.80 + 3.68–3.60 (4H, dm, CH_2—N). ^{13}C NMR ($CDCl_3$) δ (ppm): 166.0 (s), 163,9 (s), 148.6 (s), 148.0 (s), 146.5 (s), 139.6 (s), 131.5 (d), 131,3 (d), 126,5 (d), 125,6 (d), 125,3 (d), 53,9 (t), 39,4 (t). MS (EI): M^+ calcd for $C_{25}H_{19}N_5O_{10}$ 549.1132. Found: 549.1132. Anal. Calc. for $C_{25}H_{19}N_5O_{10}\cdot 1/2H_2O\cdot CH_3OH$: C, 52.88%; H, 4.04%; N, 11.86%. Found: C, 52.59%; H, 3.69%; N, 11.67%.

Synthesis of dinitromacrocycle **2**

By the same procedure, N,N′-bis(2-hydroxyethyl)-N,N′-dimethyl-2,6-pyridinedicarboxamide **8** and 4,4′-dinitrobiphenyl-2,2′-dicarbonyl dichloride afforded macrocycle **2** (0.238 g, 41%) as a white solid; mp 118–120 °C. IR (KBr) ν_{max}: 3100 (Ar—H), 2930 (CH_3, CH_2), 1745 (C=O), 1680 (N—C=O), 1630 (O—N=O), 1575 (NO_2), 1300—1050 (COO, NO_2) cm^{-1}. ^1H NMR ($CDCl_3$) δ (ppm): 8.94, 8.81, 8.79 (2H, 3 × d, J = 2.4, 2.3, 2.5 Hz, Ar—H), 8.47, 8.42, 8.40 (2H, 3 × dd, J_1 = 8.5, 8.5, 8.5 Hz, J_2 = 2.5, 2.5, 2.5 Hz, Ar—H), 7.95-7.64 (3 H, m, Py—H), 7.47, 7.15, 7.41 (2H, 3 × d, J = 8.5, 8.5, 8.4 Hz, Ar—H), 4.90–4.10 (4H, m, CH_2—O), 3.96–3.46 (4H, m, CH_2—N), 3.26, 3.11, 2.96 (6H, 3 × s, CH_3—N). ^{13}C NMR ($CDCl_3$) δ (ppm): 163.4, 163.1, 162.5 (s), 159.9, 159.7, 159.0 (s), 147.4, 146.8, 146.1 (s), 142.9, 142.7, 142.6 (s), 142.6, 141.9, 141,7 (s), 133.6, 133.3 (s), 126.6, 126.2, 125.9 (d), 125.8, 125.4, 125.0 (d), 121.9, 121.7, 121.5 (d), 121.4, 120.8, 120.4 (d), 119.7, 119.4, 119.3 (d), 59.6, 59.0, 57.8 (t), 44.0, 43.4, 43.0 (t), 34.5, 34.1, 30.6 (q). MS(FAB): M^+ + 1 calcd for $C_{27}H_{23}N_5O_{10}$: 578.1523 Found: 578.1524. Anal. Calc. for $C27H_{23}N_5O_{10}\cdot CH_3OH$: C, 4.29%; H, 4.83%; N, 10.92%. Found: C, 54.24%; H, 4.88%; N, 10.80%.

Synthesis of bis(N,N-dimethylamino)macrocycle **3**. *General procedure*

A heterogenous solution of dinitromacrocycle **1** (0.3 g, 0.55 mmol), formaldehyde (0.3 ml, 30% solution in H_2O), and 10% Pd-C (0.1 g) in absolute ethanol (50 ml) was stirred under H_2 atmosphere at room temperature for 45 min. The reaction mixture was filtered and the ethanolic solution separated; then the solid was washed with 10% HCl. The aqueous layer was carefully basified with K_2CO_3, extracted with AcOEt (3 × 25 ml) and washed with brine. The two organic solutions were jointed and dried over Na_2SO_4. The solvent was distilled off to give the macrocycle **3** as a yellow solid (0.243 g, 81%); mp 227–230 °C (CH_3OH). IR (KBr) ν_{max}: 3350 (NH), 3140 (Ar—H), 2935, 2800 (CH_3, CH_2), 1710 (C=O), 1670 (N—C=O), 1575 (C=C), 1250 (C—O) cm^{-1}. ^1H NMR ($CDCl_3$) δ (ppm): 8.19 (2H, d, J = 7.7 Hz, Py—H), 7.93 (1H, t, J = 7.3 Hz, Py—H), 7.04 (2H, d, J = 2.8 Hz, Ar—H), 6.98 (2H, d, J = 8.5, Ar—H), 6.75 (2H, dd, J_1 = 2.8 Hz, J_2 = 8.7 Hz. Ar—H), 4.26–4.14 (4H, m, CH_2O), 3.88–3.77 (2H, m, CH_2N), 3.15–3.05 (2H, m, CH_2N), 2.89 (6H, s, CH_3—N). ^{13}C NMR ($CDCl_3$) δ (ppm): 170.2 (s), 163.6 (s), 149.5 (s), 148.7 (s), 139.5 (s), 132.2 (s), 131.0 (d), 129.7 (d), 125.1 (d), 115.2 (d), 113.0 (d), 64.6 (t), 40.9 (t), 38.9 (q). MS(FAB): M^+ calcd for $C_{29}H_{31}N_5O_6$: 545.2274 Found: 545.2276. Anal. Calc. for $C_{29}H_{31}N_5O_6\cdot 1/2H_2O\cdot CH_3OH$: C, 61.43%; H, 6.14%; N, 11.94%. Found: C, 61.16%; H, 5.97%; N, 11.78%.

Synthesis of bis(N,N-dimethylamino)macrocycle **4**

Following the general procedure, dinitromacrocycle **2** afforded macrocycle **4** (0.268 g, 85%); mp 127–129 °C; IR (KBr) ν_{max}: 3140 (Ar—H), 2940, 2900 (CH_3, CH_2), 1710 (C=O), 1670 (N—C=O), 1580 (C=C), 1250 (C—O) cm^{-1}. ^1H NMR ($CDCl_3$) δ (ppm): 7.92–7.57 (3H, m, Py—H), 7.17 (d, J = 2.8 Hz, Ar—Ha), 7.12–7.08 (m, 2 H, Ar—Ha,c,a), 6.97, 6.92 (2 × d, J = 8.5, 8.7 Hz, Ar—Hc), 6.82, 6.70 (2H, dd and dm, J_1 = 8.5 Hz, J_2 = 2.8 Hz, Ar—Hb), 4.52–4.16 (6H, m, 2 × CH_2O and 2 × CH_AN), 4.06–3.83 (2H, m, 2 × CH_BN), 3.15, 3.01, 2.94 (6H, s, CH_3NCO), 2.93, 2.83, 2.75 (12H, s, CH_3N). ^{13}C NMR ($CDCl_3$) δ (ppm): 169.1 (s), 168.3 (s), 167.7 (s), 167.2 (s), 152.5 (s), 152.1 (s), 151.1 (d), 149.1 (s), 149.0 (s), 131.7 (s), 131.4 (s), 131.1 (d), 130.7 (d), 130.0 (s) 129.7 (s), 126.5 (d), 126.2 (d), 115.4 (d), 114.9 (d), 113.1 (d), 113.1 (d), 61.7 (t), 49.6 (t), 47.5 (t), 40.9 (q), 40.9 (q), 38.3 (q), 35.8 (q). MS (FAB): M^+ + 1 calcd for $C_{31}H_{36}N_5O_6$: 574.2665 Found: 574.2651. Anal. Calc. for $C_{31}H_{35}N_5O_6\cdot CH_3OH$: C, 63.47%; H, 6.40%; N, 11.39%. Found: C, 63.48%; H, 6.68%; N, 11.57%.

Electrochemical determinations

Electrochemical measurements were performed at room temperature (298(1) K) in a conventional three-electrode cell under argon atmosphere in dry CH_3CN. Tetrabuthylammonium hexafluorophosphate (0.10 M) was used as a supporting electrolyte. Experiments were performed using a BAS CV 50 W equipment with a BAS MF2012 glassy carbon working electrode (GCE) (geometrical area 0.071 cm^2), a platinum wire auxiliary electrode and a AgCl (3M NaCl)/Ag reference electrode separated from the test solution by a salt bridge containing only a supporting electrolyte. The potential of such a reference electrode was −35 mV vs. the saturated calomel reference electrode (SCE). Prior to the series of runs the working electrode was cleaned, polished and activated as reported elsewhere [7].

X-ray structure analysis

Information concerning crystallographic data collection and refinement for compound **1** are summarized in Table 3.

Intensity measurements were made on an Enraf-Nonius CAD4 diffractometer using a colourless prismatic single crystal of dimensions 0.55 × 0.18 × 0.12 mm. Graphite-monochromated Mo-Kα radiation (λ = 0.71073 Å) and ω-scan technique was used. Data collection was carried out at room temperature. Three reference reflections were measured every two hours as an intensity and orientation check and no significant fluctuation was noticed during the collection of the data. Lorentz-polarization correction was made. The crystal structure was solved by directs methods using the SHELXS system [8] and refined by full-matrix least-squares techniques [9] on F^2. The non-hydrogen atoms were refined anisotropically. All the hydrogen atoms were found by Fourier synthesis in the refinement process and only the hydrogen atoms of the acetonitrile molecule were geometrically constructed with the SHELXL-93 program with fixed isotropic displacements parameters. Geometrical calculations were performed by using PARST [10]; in Table 4 a selection of geometric parameters is shown. Figures 1 and 2 show a view of the molecular structure with crystallographic numbering scheme and a stereoscopic view of its crystal packing, respectively. Figure 1 was made with ORTEP [11] with thermal ellipsoids set at a 50% probability level and Figure 2 was made with PLUTON [12].

It is possible to obtain additional material to this paper (fractional atomic coordinates with standard deviations and equivalent isotropic temperature factors U(eq), anisotropic displacement parameters for non-hydrogen atoms, a complete table of bond lengths and angles, torsion angles and hydrogen atom coordinates) referring to deposit number CCDC-183837, author names and article quotation at the Cambridge Crystallographic Data Centre, CCDC, 12 Union Road, Cambridge CB2 1EZ, United Kingdom. The list of F_0/F_c structure data is available directly from the author until one year after the paper is published.

Results and discussion

Synthesis

The studied compounds (Chart 1) contain pyridine, amide and ester units that increase rigidity of the cavity and the whole molecule, thus allowing the study of the stereochemistry of the complexation process. On the other hand, the preparation of **2** and **4** allows to compare the role of amide hydrogen and methyl substituents on their stereochemistry and complexation.

The preparation of compounds **1** and **2** was accomplished by the method outlined in Scheme 1. Treatment of 4,4′-dinitro-2,2′-diphenic acid **5** with thionyl chloride produced dichloride **6**. Cyclisation of **6** with the appropriate diols [13] **7** and **8** under high dilution conditions provided cyclic ligands **1** and **2**, respectively. Compounds **1** and **2** were converted into **3** and **4**, respectively, by reaction with formaldehyde under reducing conditions (H_2 and Pd(C)) [14].

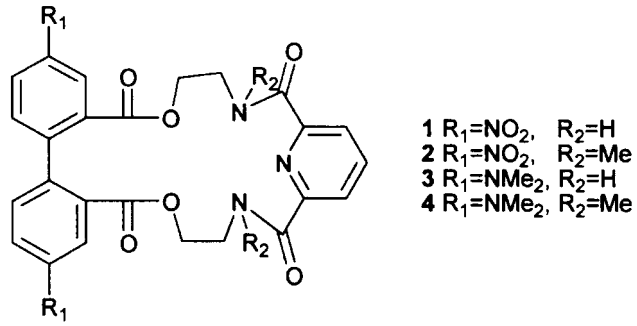

Chart 1.

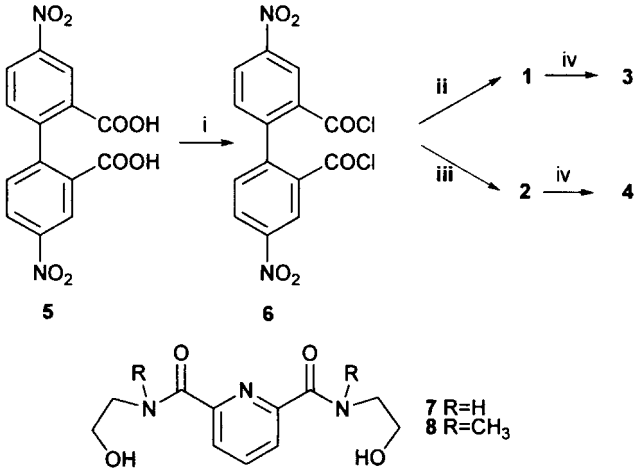

i: Cl_2SO, ii: **7**/CH_2Cl_2, iii: **8**/CH_2Cl_2, iv: H_2CO 30%, EtOH, Pd/C

Scheme 1.

Conformational analysis

The prepared macrocycles have two amide units in the ring and would constitute three conformational isomers: cisoid-cisoid, transoid-transoid and cisoid-transoid (Chart 2). The macrocycles **1** and **3** have two amide NH units; their ^{1}H NMR spectra show the expected multiplicity of signals for OCH_2- and NCH_2-. Their ^{13}C NMR spectra show single peaks for each chemically equivalent carbon indicating symmetrical structure and lack of conformational isomerism. The appearance of a downfield NH signal in these compounds shows the presence of N_{py}—NH_{amide} intramolecular hydrogen bonding and therefore cisoid-cisoid conformation.

Macrocycle **2** shows in its ^{1}H NMR spectrum three N—CH_3 (1 : 1.5 : 1) signals and three sets of aromatic signals in the same ratio. Therefore, the presence of the relatively bulky methyl substituents on amide N in this compound leads to restricted rotation around amide bond and generates three conformers. ^{1}H NMR experiments carried out in DMSO at 100 °C demonstrated that under these conditions the signals corresponding to each conformer collapse to broad singlets. In addition, one of the conformers is asymmetrical as the number of observed signals shows the presence of non-equivalent hydrogen atoms.

Compound **4** also shows in ^{1}H NMR three possible conformations because three different $N(CH_3)_2$ signals are observed (2 : 1 : 2 ratio). When the $CONCH_3$ peaks were

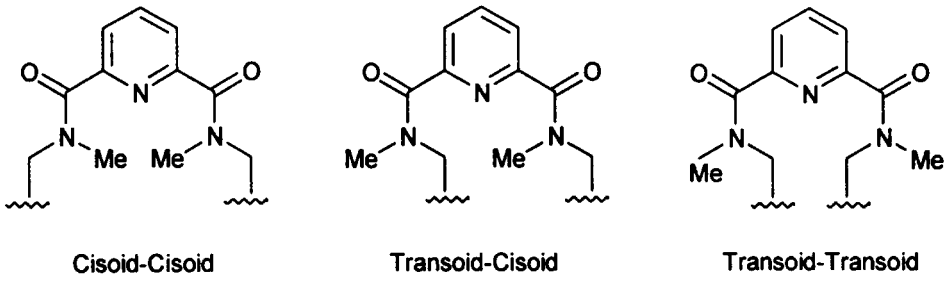

Chart 2.

Table 1. Hydrogen bond geometry for **1**·CH_3CN

D—H···A	d(H···A) (Å)	d(D···A) (Å)	(D—H···A) (°)
N3—H3N···N2	2.26(3)	2.699(4)	108(2)
N1—H1N···N2	2.21(3)	2.708(3)	110(2)
N3—H3N···N55	2.48(3)	3.321(4)	152(2)
N1—H1N···N55	2.35(3)	3.080(5)	136(3)
N3—H3N···O5	2.69(3)	2.695(3)	80(2)

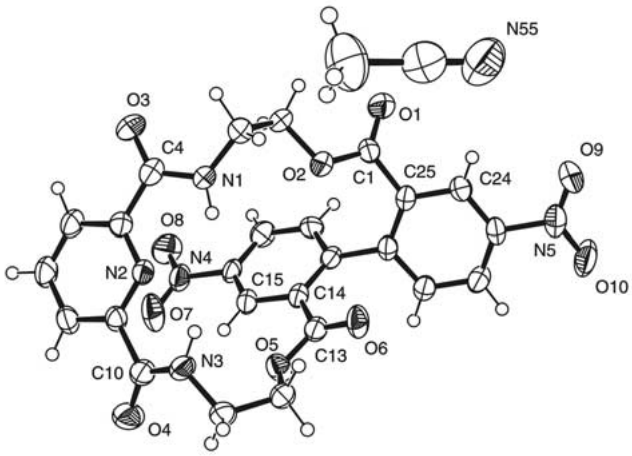

Figure 1. Molecular structure with crystallographic numbering scheme for **1**·CH_3CN.

studied it was observed that the minor conformation shows different signals for each $CONCH_3$ group. It was clear also that both meta H in the pyridine ring are not chemically equivalent and that they are present as different signals in the spectrum. Similarly to compound **2**, when the ^1H NMR experiments are carried out in DMSO at 100 °C broad signals are observed, which means that the system is close to coalescence temperature. Additionally, triplicity of most of the signals corresponding to the carbon atoms in ^{13}C NMR spectra for both compounds **2** and **4** are found. Thus, it is reasonable to accept that compounds **2** and **4** exist in three possible conformations: cisoid-cisoid, transoid-transoid and cisoid-transoid.

Crystal structure of **1**

X-ray single-crystal studies were performed on compound **1**. Suitable crystals were obtained by slow diffusion of acetonitrile into a solution of the compound in methanol. Ligand **1** crystallizes with a molecule of acetonitrile. The amide groups N(3)—C(10)—O(4) and N(1)—C(4)—O(3) are twisted by 15.39 (0.47) and 9.88(0.49) with respect to the pyridine ring lying on opposite sides of the mean plane of the pyridine ring. The two amide nitrogens point inward and amide oxygens point outward the cavity. Conformation of the macrocycle is stiffened by intramolecular hydrogen bonds (NH_{amide} · N_{py}) (Table 1). The presence of such hydrogen bonds is known to stabilise flat syn-syn conformations for compounds containing 2,6-dicarbamoylpyridine moieties [15]. Additionally, hydrogen bonds are also observed between N—H_{amide} and the acetonitrile molecule.

The biphenyl unit shows a smaller dihedral angle between the aromatic rings (62.5°) than in other related compounds in which the benzene nuclei are almost perpendicular [4]. On the other hand, the ester carbonyl groups are not equivalent in their conformation. Thus, one of these groups is almost coplanar in relation to the corresponding aromatic ring (biphenyl) (O(6)—C(13)—C(14)—C(15) = 167.92°) whereas another is clearly outside the plane (O(1)—C(1)—C(25)—C(24) = 36.98°). Finally, the pyridine ring is close to one of the aromatic rings of biphenyl, with the dihedral angle between both rings around 38°. In conclusion, the cavity is bent in such a way that the free space inside is very small. Even though the acetonitrile molecule is outside the cavity it could hinder the cation approach.

Complexation experiments

Complexation experiments were carried out with ligands **1-4** and $Zn(NO_3)_2$, $Cd(NO_3)_2$ and $Hg(CN)_2$ and complexation constants in CD_3CN were determined by using ^1H NMR techniques (Table 2). With compounds **1** and **3** different signals for ligands and their complexes were observed whereas complexation with **2** and **4** was studied using titration experiments On the basis of NMR-based structural studies, the macrocycles **1–4** can be classified into (a) macrocycles possessing amide NH units (**1** and **3**) and (b) macrocycles possessing amide N—CH_3 units and having several conformations in solution (**2** and **4**).

Macrocycles **1** and **3** with N_{py}—NH_{amide} intramolecular hydrogen bonding show very low complexation constants (log *K* from 1.9 to 1.5). This behavior could be related to the hydrogen bond that makes the pyridine nitrogen unsuitable for complexing. However, the complex formed between **1** and $Hg(CN)_2$ is of particular interest. This complex shows

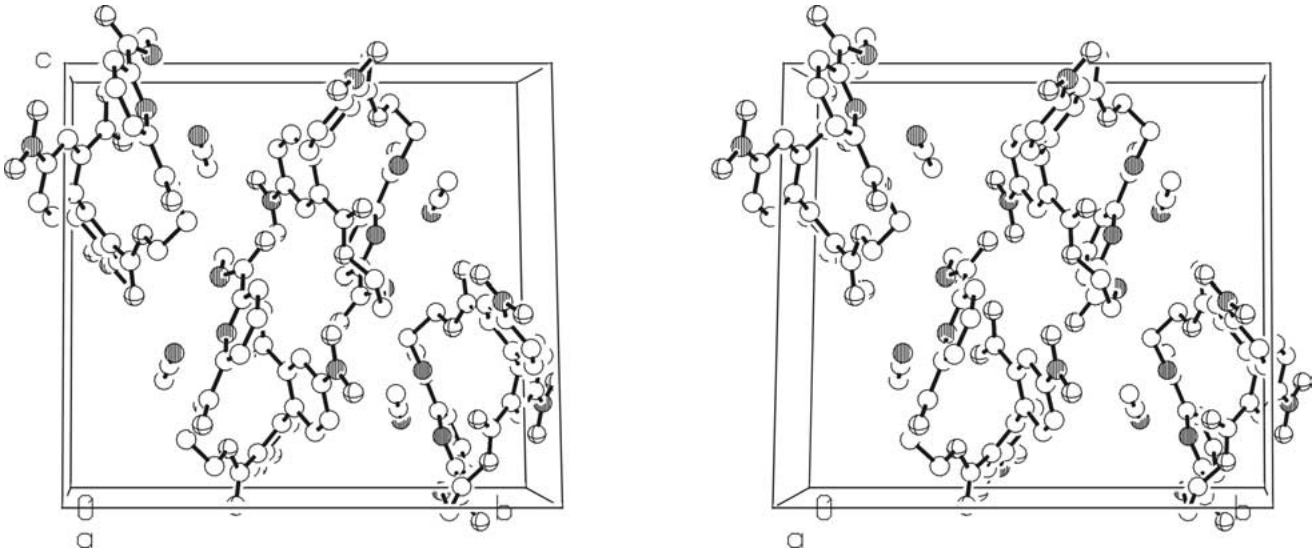

Figure 2. View of molecular structure for **1**·CH_3CN.

Table 2. Log *K* for **1–4** in CH_3CN

Ligand	Log *K*		
	$Zn(NO_3)_2$	$Cd(NO_3)_2$	$Hg(CN)_2$
1	1.8	1.9	1.6
2	0.6	0.8	–
3	1.5	1.6	–
4	1.9	2.2	–

Table 3. Crystal data and structure refinement for **1**

Empirical formula	$C_{25}H_{19}N_5O_{10}$ + $NCCH_3$
Formula weight	590.51
Temperature	293(2) K
Wavelength	0.71073 Å
Crystal system	Monoclinic
Space group	P21/n
Unit cell dimensions	a = 10.6422(5) Å alpha = 90 deg.
	b = 16.6551(5) Å beta = 101.06(5) deg.
	c = 15.2908(5) Å gamma = 90 deg.
Volume	2659.9(2) $Å^3$
Z	4
Density (calculated)	1.475 Mg/m^3
Absorption coefficient	0.115 mm^{-1}
F(000)	1224
Crystal size	0.55 × 0.18 × 0.12 mm
Theta range for data collection	2.30 to 26.24 deg.
Index ranges	$0 \Leftarrow h \Leftarrow 13, -20 \Leftarrow k \Leftarrow 0, -19$
	$\Leftarrow l \Leftarrow 18$
Reflections collected	5660
Independent reflections	5367 [R(int) = 0.0969]
Refinement method	Full-matrix least-squares on F^2
Data/restraints/parameters	5362/0/464
Goodness-of-fit on F^2	0.776
Final R indices [I>2sigma(I)]	R1 = 0.0493, wR2 = 0.0898
R indices (all data)	R1 = 0.1831, wR2 = 0.1090
Largest diff. peak and hole	0.199 and −0.234 e.$Å^{-3}$

in ^1H NMR that both aromatic rings of the biphenyl residue are not equivalent probably due to the position of both CN groups in the space that affects each ring in a different way. This hypothesis agrees with the observation of different models.

Compounds **2** and **4** in which there are no intramolecular hydrogen bonds were expected to show better complexation ability. However, it was found that they do not complex $Hg(CN)_2$; $Zn(NO_3)_2$ and $Cd(NO_3)_2$ give rise to very low values (log *K* from 2.2 to 0.6). An explanation for this behavior is strong steric hindrance caused by both methyl groups for the cation entering the cavity. Complexes formed by these ligands showed a fast exchange on the NMR time scale and shifts of the signals were observed. However, it should be noted that one of the conformations present in solution experiments stronger shifts than the other conformations even though the ratio between the three species keeps the same value (see Figure 3 as an example). Moreover, in compound **2** the most affected species is the asymmetric conformation whereas in compound **4** is one of the symmetric conformations which is widely modified by complexation.

Electrochemical studies

(a) Electrochemistry of **1** and **3**

In Figure 4 typical CVs of solutions of (a) **3** and (b) **1** in CH_3CN are presented. As depicted in Figure 4a, the anodic scanning revealed three overlapping peaks at +835 (A1), +995 (A2) and +1155 (A3) mV for **3**, coupled in the subsequent cathodic scan by cathodic peaks at +1080 (C3), +890 (C2) y +685 (C1) mV. At more cathodic potentials, as well as in CVs initiated cathodically at 0 V, two prominent reduction peaks appear at −915 (C4) and −1520 (C5) mV, coupled with ill-defined anodic peaks at −1260 (A5) and −570 (A4) mV. An ill-defined wave near −700 mV (C6) precedes peak C4.

This response can be described in terms of the superposition of electrode processes involving different electroactive

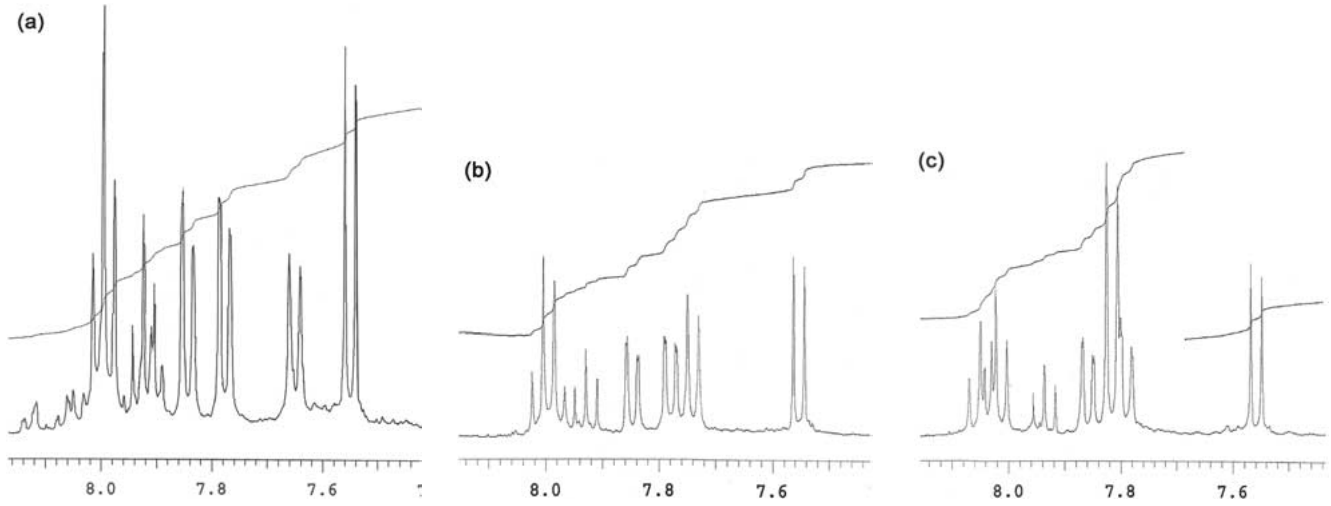

Figure 3. Titration experiment of **4** with $Cd(NO_3)_2$ in CD_3CN. (a) 0 equivalents of $Cd(NO_3)_2$, (b) 0.75 equivalents of $Cd(NO_3)_2$, (c) 2 equivalents of $Cd(NO_3)_2$.

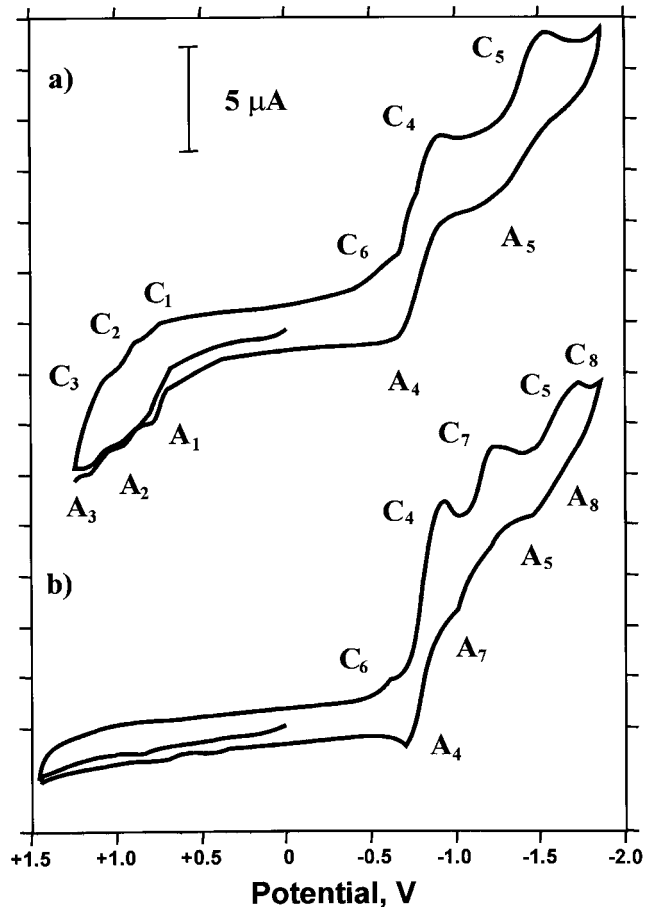

Figure 4. Cyclic voltammograms initiated in the anodic direction at the GCE of 0.30 mM solutions of (a) **3**, (b) **1** in MeCN (0.10 M Bu_4NPF_6). Potential scan rate 100 mV/s.

centers in molecule **3**. Thus, the couples C4/A4 and C5/A5 must correspond to successive one-electron transfer processes involving the biphenyl moiety. These are essentially reversible processes in which a radical anion and a dianion are formed [16, 17]:

$$\mathrm{BiPh} + e^- = \mathrm{BiPh}^{\cdot -} \quad \mathrm{BiPh} = \text{Biphenil} \qquad (1)$$

$$\mathrm{BiPh}^{\cdot -} + e^- = \mathrm{BiPh}^{2-}. \qquad (2)$$

The last species, however, are sensitive to protonic impurities and/or traces of water. Their presence results in a decrease of the anodic currents.

Following a similar scheme, couples C1/A1, C2/A2 y C3/A3 are attributable to the oxidation of the biphenyl group, forming successively a radical cation and a dication. These processes are mediated, however, by the nucleophilic attack of the solvent and/or water, resulting in the appearance of a complicated electrochemical pattern [18–21]. The peak A6 can be assigned to the proton-assisted reduction of the pyridine moiety [22].

The voltammetric response of **1** was similar. As shown in Figure 4b, the initial reduction of biphenyl groups (C4) at −935 mV is followed by reduction peaks at −1235 (C7), −1580 (C5) and −1830 (C8) coupled with ill-defined anodic counterparts. A weak wave (C6) also appears preceding the peak C4, while in the positive region of potentials, the C1/A1, C2/A2 and C3/A3 couples are absent. Comparing the response of **1** with that of **3**, it is reasonable to attribute the peak at −1580 mV to the second electron transfer to the biphenyl unit (peak C5); peaks at −1235 (C7) and −1830 (C8) can be assigned to the reduction of nitro groups. This involves two successive one-electron transfers which can be represented as [23–25]:

$$\text{R-NO}_2 + e^- = \text{R-NO}_2^{\cdot -} \qquad (3)$$

$$\text{R-NO}_2^{\cdot -} + e^- = \text{R-NO}_2^{2-}. \qquad (4)$$

The electrochemical response obtained for biphenyl moieties in both ligands is similar. This suggests that the substituents have little influence on the electrochemistry of such systems.

(b) Electrochemistry of Cu^{2+}-**1** system

A typical CV of Cu(II) acetate solutions in CH_3CN is shown in Figure 5a. Cathodic peaks at −445 (C9) and −1300 mV

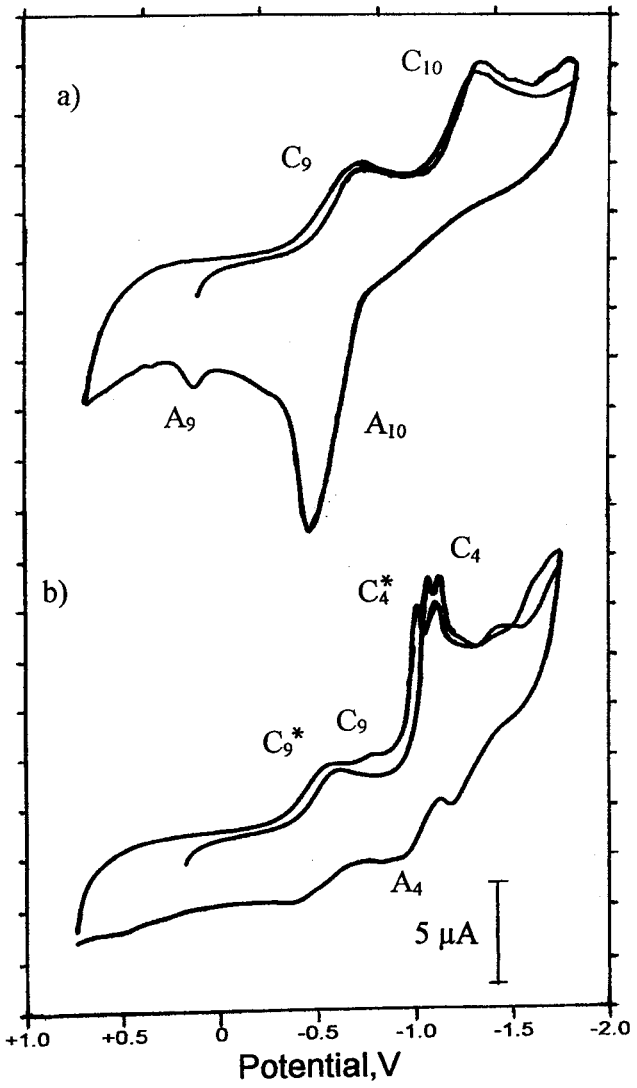

Figure 5. CVs at the GCE of (a) $Cu(CH_3COO)_2$ (0.70 mM); (b) $Cu(CH_3COO)_2$ (0.70 mM) plus **1** (0.58 mM) solutions in MeCN (0.10 M Bu_4NPF_6). Potential scan rate 100 mV/s.

(C10) appear coupled with anodic ones at −150 (A10) and +480 mV (A9). This response corresponds to the stepwise reduction of Cu^{2+} ions to metallic copper via two successive one-electron transfer processes. The presence of two separated electrode processes for Cu^{2+} reduction is consistent with the recognized stabilization of Cu^{+} ions by CH_3CN [26]. In agreement with that scheme, the peak A10 presents a typical tall shape, characteristic of stripping oxidations of metallic layers.

Upon addition of increasing amounts of **1**, the voltammetric pattern changes progressively, the metal-centered electrode processes being superimposed on the ligand-centered processes. As shown in Figure 5b, the peak current of the initial one-electron reduction of Cu^{2+} slightly decreases while the second reduction step (peak C10) decreases and is shifted towards more negative values. The stripping oxidation A10 disappears, suggesting that formation of free copper at potentials near to −1500 mV is followed by a comproportionation reaction with the parent Cu(II) complex yielding stable Cu(I) species.

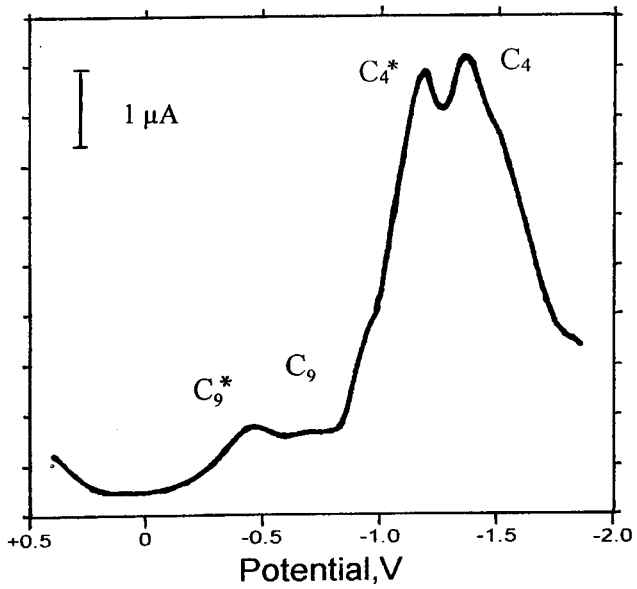

Figure 6. Square wave voltammogram initiated in the cathodic direction at the GCE of a $Cu(CH_3COO)_2$ (0.70 mM) plus **1** (1.16 mM) solution in MeCN (0.10 M Bu_4NPF_6). Potential step 4 mV; square wave amplitude 25 mV; frequency 15 Hz.

Interestingly, the peak C4 is shifted towards more negative values and resolved in two peaks at −895 and −945 mV (C4* and C4, respectively), whose relative height depends on the ligand-to-metal molar ratio. Since this dual response can be attributed to the reduction of 'free' and 'coordinated' biphenyl units, one can conclude that the coordination with copper ions facilitates the electrochemical reduction of such groups. A similar resolution was observed in the peak C9, corresponding to the reduction of 'free' and 'coordinated' (peak C9*) Cu^{2+} ions, as can be seen in SQWVs shown in Figure 6. The electrode processes can be schematized as:

$$Cu(II)\mathbf{1}^{2+} + e^{-} = Cu(I)\mathbf{1}^{+} \quad (5)$$

$$Cu(I)\mathbf{1}^{+} + e = Cu^{\circ} + \mathbf{1} \quad (6)$$

The formation of a Cu^{2+}-**1** complex was monitored by the increase in the peak current of peak C4* in solutions containing a constant concentration of Cu^{2+} and increasing concentrations of **1**. As expected, the height of peak C4* tends to a limiting value allowing for the determination of the stoichiometry of the complex and its stability constant, K, by applying the generalized molar-ratio method, following the scheme already described [27, 28]. A 1 : 1 Cu^{2+} : **1**1 stoichiometry was found with K = 1.02 (0.02)10^3 M^{-1}.

(c) Electrochemistry of the Cu^{2+}-**3** system

Upon addition of increasing amounts of **3** to a solution of $Cu(CH_3COO)_2$, the voltammetric pattern changes more drastically than in the case of **1**. Although the voltammetric pattern is considerably complicated for low ligand-to-metal ratios, for molar ratios close to unity it becomes as depicted in Figure 7. A well-defined reduction peak (C11) appears at −625 mV accompanied by a prominent stripping peak (A11) near −100 mV. These peaks obscure the remaining

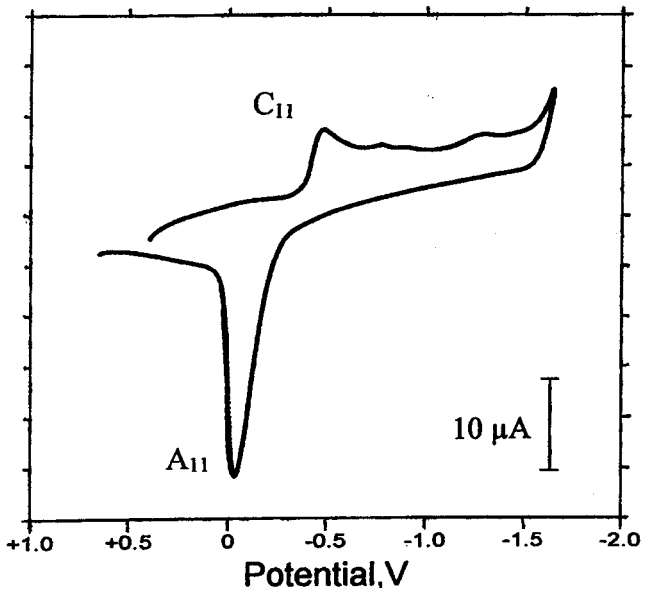

Figure 7. Cyclic voltammogram at the GCE of a $Cu(CH_3COO)_2$ (0.70 mM) plus **3** (2.18 mM) solution in MeCN (0.10 M Bu_4NPF_6). Potential scan rate 100 mV/s.

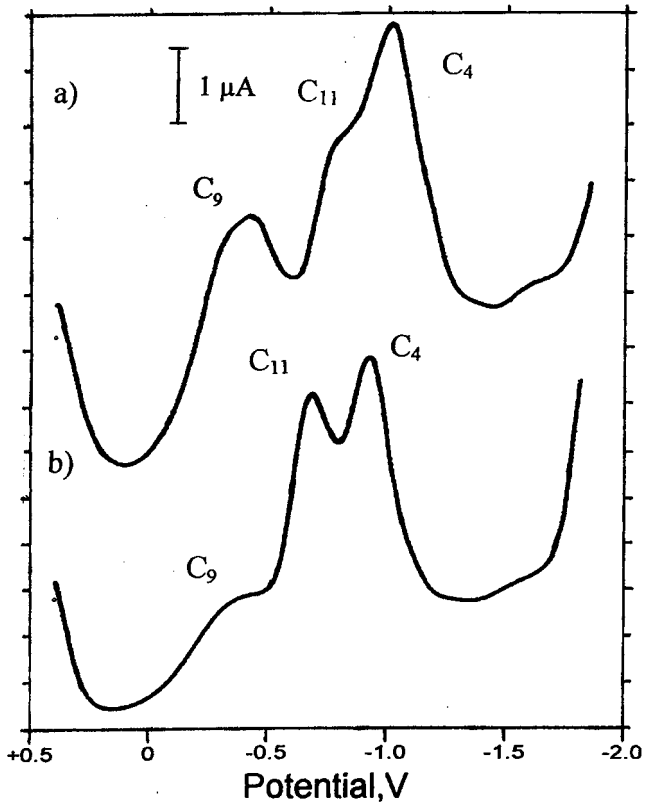

Figure 8. SQWVs at the GCE initiated in the cathodic direction of a $Cu(CH_3COO)_2$ (0.70 mM) plus (a) 0.38 mM **3**; (b) 1.12 mM **3** solutions in MeCN (0.10 M Bu_4NPF_6). Potential step 4 mV; square wave amplitude 25 mV; frequency 15 Hz.

ligand-centered electrochemical processes and their height is approximately twice of that of peaks C9 (or C10) and A10, respectively. This behavior can be interpreted assuming that upon complexation with **3** the Cu(I) oxidation state is largely destabilized and in such a way the reduction of the Cu(II)-**3** complex takes place in a two-electron step:

$$\text{Cu(II)}\mathbf{3}^{2+} + 2e^- = \text{Cu}^\circ + \mathbf{3}. \qquad (7)$$

The variation of the voltammetric response on the ligand-to-metal ratio is illustrated in SQWVs in Figure 8. On increasing the $\mathbf{3}/Cu^{2+}$ molar ratio, the two-electron reduction of the metal center (peak C11) replaces progressively the one-electron reduction of uncomplexed Cu^{2+} (peak C9). The complexation was monitored by the increase in the peak current of C11 which, as expected, tends to a limiting value for solutions containing an excess of ligand. The application of the generalized molar-ratio method provides a value of the stability constant of $K = 1.36(0.04)10^3\ M^{-1}$.

As can be seen in SQWVs in Figure 8, the peak C4 is not resolved in two separated peaks whereas the ligand-centered processes occurring at potentials more negative than peak C4 become considerably decreased in sharp contrast with the observations in the case of **3**. These observations are consistent with the foregoing considerations. By the first taken, since the process C4 appears after the reduction of Cu(II) to metallic copper, only 'free' ligand remains as a responsible of that peak. By the second, the formation of a metallic layer of Cu on the electrode surface presumably results in a decrease of the electrode sensitivity towards electron transfer processes.

The difference in the electrochemical response of the Cu^{2+}-**3** and Cu^{2+}-**1** complexes can in principle be discussed in the light of the recognized preference of Cu^+ to acquire tetrahedral or pseudo-tetrahedral geometries [29, 30]. Thus, formation of a stable Cu^+-**1** complex requires presumably coordination with one of the nitro groups through one of its oxygen atoms. In the case of **3**, a similar situation is not possible due to the spatial position of the lone electron pair of the nitrogen atoms bound to the biphenyl moiety. Thus, complexation of copper ions by **1** determines a stabilization of the Cu(I) oxidation state with respect to its disproportionation into Cu(II) and Cu(0). In contrast, complexation of copper ions with **3** yields to a large destabilization of such an intermediate oxidation state.

Acknowledgments

We thank the Dirección General de Enseñanza Superior e Investigación Científica (PB98-1430-C02-01, PB98-1430-C02-02) for support. M.J. Bañuls is grateful to the Generalitat Valenciana for a predoctoral fellowship. L.E. Ochando and F.J. Tamarit are grateful to J. Rius and M. Font (ICMAB-CSIC) for their help in data collection.

References

1. J. Rebek Jr., R.V. Wattley, T. Costello, R. Gadwood, and L. Marsshall: *Angew. Chem. Int. Ed. Engl.* **20**, 584 (1981).
2. Y. Rubin, K. Dick, F. Diererich, and T.M Georgiadis: *J. Org. Chem.* **51**, 3270 (1986).
3. S.A. McFarland and N.S. Finney: *J. Am. Chem. Soc.* **123**, 1260 (2001).
4. A.M. Costero, C. Andreu, R. Martínez-Máñez, J. Soto, L.E. Ochando, and J.M. Amigó: *Tetrahedron* **54**, 8159 (1998).

5. A.M. Costero, R. Andreu, E. Monrabal, R. Martínez-Máñez, F. Sancenón, and J. Soto: *J. Chem. Soc., Dalton Trans*. (2002), in press.
6. S. Kumar, N. Kaur, and H. Singh: *Tetrahedron* **52**, 13483 (1996).
7. A. Doménech, E. García-España, P. Navarro, and F. Reviriego: *Talanta* **51**, 625 (2000).
8. G.M. Sheldrick: Shelxs86, Program for the crystal structure determination, University of Cambridge, England.
9. G.M. Sheldrick: Shelxl93, Program for the crystal structure refinement, University of Göttingen, Germany.
10. M. Nardelli: Parst95, Program for geometrical calculations, *Comput. Chem.* **7**, 95–98 (1983).
11. L.J. Farrugia: ORTEP-3 for Windows v1.05, Dept. of Chemistry, University of Glasgow (1999).
12. A.L. Spek: Pluton92, Program for molecular graphics, University of Utrech, The Netherlands.
13. S. Kumar, M.S. Hundal, N. Kaur, R. Singh, H. Singh, G. Hundal, M.M. Ripoll, and J.S. Aparicio: *J. Org. Chem.* **61**, 7819 (1996).
14. M.G. Romanelli and E.I. Becker: *Org. Synth. Coll.* **V**, 552.
15. C.A. Hunter and D.A. Purvis: *Angew. Chem. Int. Ed. Engl.* **104**, 792 (1992)
16. A.C. Aten, C. Buthker and G.J. Hoijtink: *J. Chem. Soc. Faraday Trans.* **55**, 324 (1959).
17. R.D. Allendoerfer and P.H. Rieger: *J. Am. Chem. Soc.* **87**, 2336 (1965). L.R. Faulkner and A.J. Bard: *J. Am. Chem. Soc.* **90**, 6284 (1968). T.J. Katz, W.H. Reinmuth, and D.E. Smith: *J. Am. Chem. Soc.* **84**, 802 (1962).
18. L.S. Marcoux, J.M. Fritsch, and R.N. Adams: *J. Am. Chem. Soc.* **89**, 5766 (1967).
19. M.E. Peover and B.S. White: *J. Electroanal. Chem.* **13**, 93 (1967).
20. E.J. Majeski, J.D. Stuart, and W.E. Ohnesorge: *J. Am. Chem. Soc.* **90**, 633 (1968).
21. V.D. Parker and L. Eberson: *J. Am. Chem. Soc.* **92**, 7488 (1970).
22. C.L. Perrin: Mechanisms of organic polarography, in P. Zuman and C.L. Perrin (eds.), *Organic Polarography, Interscience*, New York (1969), p. 280.
23. G.S. Alberts and I. Shain: *Anal. Chem.* **35**, 1859 (1963).
24. R.S. Nicholson and I. Shain: *Anal. Chem.* **37**, 190 (1965).
25. A.C. Testa and W.H. Reinmuth: *J. Phys. Chem.* **83**, 784 (1961).
26. J.F. Coetzee and W.K. Istone: *Anal. Chem.* **52**, 53 (1980).
27. A. Bianchi, A. Doménech, E. García-España, and S.V. Luis: *Anal. Chem.* **65**, 3137 (1993).
28. A. Doménech, E. García-España, and J.A. Ramírez: *Talanta* **42**, 1663 (1995).
29. W.E. Geiger: *Progr. Inorg. Chem.* **33**, 275 (1985).
30. S.K. Kano, R.S. Glass, and G.S. Wilson: *J. Am. Chem. Soc.* **115**, 592 (1993).